Analytical Cellular Pathology, 5 (1993) 353–366

© 1993 Elsevier Scientific Publishers Ireland Ltd. All rights reserved. 0921-8912/93/$06.00

ANACEL 00171

Morphometric and tridimensional studies of tubular cystic degeneration in rat kidney following exposure to cisplatin

Jacqueline Zanen, Valérie Carinci, Denis Nonclercq, Gérard Toubeau, Guy Laurent and Jeanine Anne Heuson-Stiennon

Laboratoire d'Histologie, Faculté de Médecine, Université de Mons-Hainaut, B-7000 Mons, Belgium

(Received 30 September 1992; accepted 10 February 1993)

Abstract

Cisplatin, a widely used chemotherapeutic agent, is characterized by a dose-limiting renal toxicity. Cystic tubular dilatation is the most typical histopathological alteration encountered in cisplatin-treated rats. The purpose of the present study was to explore by a morphometric approach the development of cystic degeneration and, in particular, to analyse, by computer-assisted tridimensional reconstructions, the spatial structure and the tubular origin of cisplatin-induced renal cysts. This study was performed on rats given 8 mg/kg cisplatin i.p. for four days and sacrificed 4, 7, 14, 21, 50 and 60 days after last drug administration. The relative area occupied by cystic tubules increased rapidly in the outer stripe of outer medulla (OSOM) and reached a maximum 21 days after the end of treatment. Cystic dilatations appeared later in the kidney cortex and the inner stripe of outer medulla (ISOM). The tridimensional study of cystic tubules located in OSOM confirmed previous reports indicating that they arise from proximal straight tubules and showed that cystic degeneration was not associated with atrophy or degeneration in more proximal parts of the nephron. Moreover, cystic tubules located in ISOM were found to originate from distal straight tubules and/or the loop of Henle, an observation which, to our knowledge, has not been reported so far in cisplatin-treated rats.

Key words: Renal cystic tubule; Cisplatin; Image analysis; Nephrotoxicity

Introduction

Cisplatin [*cis*-diamminedichloroplatinum (II)], an important chemotherapeutic agent, is principally used in clinics for the treatment of testicular and ovarian cancers but is also active against a variety of other human neoplasms [15,21,27,32–34]. Despite the application of preventive therapies such as hyperhydration and mannitol pretreatment to reduce nephrotoxicity [21,38], renal insufficiency is recognized as the dose-limiting toxicity of this drug [15]. The clinical manifestations of cisplatin

Correspondence to: Dr. Jacqueline Zanen, Service d'Histologie, Faculté de Médecine, Université de Mons-Hainaut 24, Avenue du Champ de Mars B-7000 MONS, Belgium.

nephrotoxicity consist of a rapid decrease in glomerular filtration rate leading to a rise in urea and serum creatinine. These physiological alterations are accompanied by an important polyuria. This phase of acute renal failure is followed by chronic renal dysfunction characterized by calcium and magnesium wasting [1,7,10,22, 24,25,35,41].

Acute and chronic renal failures due to cisplatin are associated with typical tubular alterations. Short-term clinical and animal investigations reveal that cisplatin induces an acute tubular necrosis involving mainly the pars recta of the proximal tubules (segment S3) in the outer stripe of outer medulla (OSOM) [6,12,18]. Long-term studies show that necrotic tubules degenerate progressively into cystic tubules that persist over a long period of time after drug exposure [13,14,20,28–30,37]. However, previous work mostly focused on the morphological description of this morphological alteration and did not analyse its development on a quantitative basis. Moreover, the spatial structure of cystic tubules as well as their relationships with other parts of the nephron remain largely unexplored.

The present time-course study was undertaken to evaluate, by a computer assisted morphometric approach, the evolution of cisplatin-induced cystic degeneration in rat kidneys. Moreover, a tridimensional reconstruction of cystic tubules has allowed us to obtain original data on the origin and structure of cystic tubules.

Material and Methods

Animals

All experiments were performed on female Sprague–Dawley rats weighing 180–200 g. Animals were purchased from a commercial breeding farm (Iffa Credo, l'Arbresle, France). Immediately after their arrival, they were distributed at random into seven experimental groups of four animals. During the whole duration of the study, animals were maintained in an animal facility submitted to a regular 12-h light/dark cycle and received food (Rodent chow type AO4, UAR Villemoisson-sur-Orge) and tap water ad libitum.

Treatment

Six experimental groups were exposed to cisplatin. The drug formulation used to treat animals (PLATINOL; Laboratoires Bristol Bénélux, Brussels, Belgium) was that available for clinical practice. Cisplatin was given i.p. at a daily dose of 2 mg/kg, the volume of solution delivered being calculated on the basis of body weight determined just before injection. A total dose of cisplatin (8 mg/kg) was administered by four daily consecutive injections. Rats of the different groups were terminated at selected time intervals (4, 7, 14, 21, 50 and 60 days) after the end of the treatment. In parallel, one control group received 0.9 % NaCl i.p. and was processed along with the treated rats.

Morphological methods

The animals were sacrificed by decapitation and the kidneys rapidly excised after opening of the abdominal cavity. The kidneys were bisected longitudinally and immediately fixed in Duboscq-Brazil fluid. The specimens were rinsed in 70° ethanol, dehydrated in graded ethanol and butanol and finally embedded in paraffin. The tissue blocks were sectioned at 4–5 μm on a Reichert Autocut 2040 microtome equip-

ped with a glass knife. Some samples, selected for the tridimensional analysis, were sectioned serially (approx. 160 consecutive sections of 10 μm thick). All sections were stained with periodic acid-Schiff, hemalum and luxol fast blue.

The terminology of the zones of the kidney and nephron segments is in accordance with standard abbreviations [19]. The definition of renal cyst is based on the observation of the tubular lumen and refers to the terminology used by Gardner [16].

Computer-assisted morphometric analysis

The SAMBA system (TITN-Alcatel Grenoble, France) was used to make area measurements of tubular lumens. Kidney sections were analyzed at 50 × magnification on a Zeiss Axioplan microscope connected to a color high-resolution JVC KY.15 video camera. Images of microscopic fields were digitalized, displayed on a color monitor (512 × 512 pixels) and stored on an IBM-compatible microcomputer (COMPAQ 80386 reinforced with a coprocessor 80387). After interactive selection of grey level corresponding to tubular lumens (well-defined unstained area contrasting with other kidney structures) the luminal area was automatically measured in pixels with an appropriate program. One slide per experimental animal was used for the morphometric evaluation and ten 0.763 mm^2 fields were scanned at random in kidney cortex and, similarly, in OSOM. The total luminal area was obtained by recording, for each of the ten fields, the number of pixels corresponding to the tubular lumina (total number of pixels is 262,144 for one field). These values are pooled to obtain individual values from which the area density is calculated (percentage of the total scanned area occupied by tubular lumina). The mean area density for each experimental group ($n = 4$) is then obtained from the individual values of area densities.

To calculate the frequencies of tubular profiles in OSOM, the area of each tubular lumen larger than 1000 μm^2 was recorded. A total area of 7.63 mm^2 (ten fields) was scanned for each animal. The tubular profiles located in each field were sorted according to their size and were finally distributed into 4 groups corresponding to the following size intervals: 1000–4000 μm^2, 4001–10 000 μm^2, 10 001–30 000 μm^2 and $>30\,000$ μm^2. Individual values were pooled for each experimental group ($n = 4$). The lower limit of 1000 μm^2 has been chosen arbitrarily and corresponds to 10-fold the mean luminal area of normal straight proximal tubules (observed in transverse section).

Statistical analysis

Individual values of area density recorded for each treated group were compared to control values by the non-parametric Mann-Whitney U-test.

Tridimensional reconstruction of cystic tubules

Spatial reconstructions of cystic tubules have been realized from serial kidney sections of animals sacrificed two months after cisplatin administration. Consecutive sections (10 μm thick) of renal tissue were processed at 63 × magnification by the SAMBA system. The serial images of region with a cystic tubule to be reconstructed were digitalized and printed on a printer HP laser III. The software used to visualize the architecture of cystic tubules was developed for Macintosh computers by Yves Usson (1988-Alcatel TITN-Grenoble, France). The program 'Acquisition' allows one to create the data files required for the reconstruction with a graphic tablet (an

input device that converts two dimensional information, such as drawing, into a computer readable format). The consecutive tubular profiles obtained from the digitalized microscopic images were successively recorded on a Macintosh II ci, via the graphic tablet. After interactive 'fitting' of the successive sections (glomeruli observed on successive sections were used as markers for translations and rotations), the program 'Colour reconstruction' was used to display on the screen the tridimensional view of cystic tubules. A total of seven cystic tubules chosen at random in the different zones of the kidney have been submitted to this analysis.

Results

Morphometric analysis of morphological alterations

Light microscopy examination of kidneys reveals prominent tubular injury four days after cisplatin administration. As shown in Fig. 1a, acute tubular necrosis principally involves S3 segments present in the outer stripe of outer medulla (OSOM). One week after treatment, most necrotic tubules undergo cystic dilatation. Cystic tubules which progressively develop in OSOM between 1 and 3 weeks following cisplatin treatment (Figs. 1c and 1d), are characterized by a wide lumen lined by a flattened epithelium, and exhibit a thickened basement membrane (Fig. 1b). After 2 months, cystic degeneration progresses toward the kidney cortex and the inner stripe of outer medulla (ISOM).

The development of cystic tubules has been evaluated by the morphometric analysis of the area occupied by tubular lumens in OSOM and renal cortex. Evidence of tubular dilatation appears early in OSOM since the values registered after 4 days are already statistically higher than controls. The surface occupied by cystic tubular sections reaches its maximum value 3 weeks after sacrifice. From this point and up to 60 days, the area density of tubular lumens represents 50% of OSOM tissue surface versus only 10% in control group (Table 1). Compared with OSOM, cystic tubular dilatation in kidney cortex is much less severe and appears later on (Table 1). The increase of tubular luminal area after exposure to cisplatin results from a progressive dilatation of tubules themselves. As shown in Fig. 2, the development of cisplatin-induced tubular injury in OSOM can be split into four arbitrary stages. The first stage (Fig. 2a) is observed during the first week after cisplatin treatment and corresponds to the acute tubular necrosis which precedes cystic dilatation. After epithelium desquamation, all necrotic tubules exhibit a wide lumen (approx. 1000–4000 μm^2) lined by a denuded basement membrane. During the second stage (second week after treatment), the number of necrotic tubule decreases. This phenomenon is due to some extent to a repair of necrotic tubules, but mostly results from a progressive degeneration into microcystic tubules. As shown in Fig. 2b, microcystic tubules (lumen area between 4000 and 10 000 μm^2) are prominent during the two first weeks after the treatment. The third stage (Fig. 2c) corresponds to the progressive dilatation of *microcystic* tubules into medium size cystic tubules (lumen area between 10 000 and 30 000 μm^2). The latter reach a maximum value 21 days after the end of the treatment. The fourth stage, which develops 1–2 months after cisplatin administration is characterized by the development in OSOM of true renal cysts with a diameter >200 μm (lumen area $>30\,000$ μm^2) (Fig. 2d). Animals sacrificed two months after cisplatin injection present a significant increase of renal cysts as compared to those observed at one month. Some renal cysts have a luminal area superior

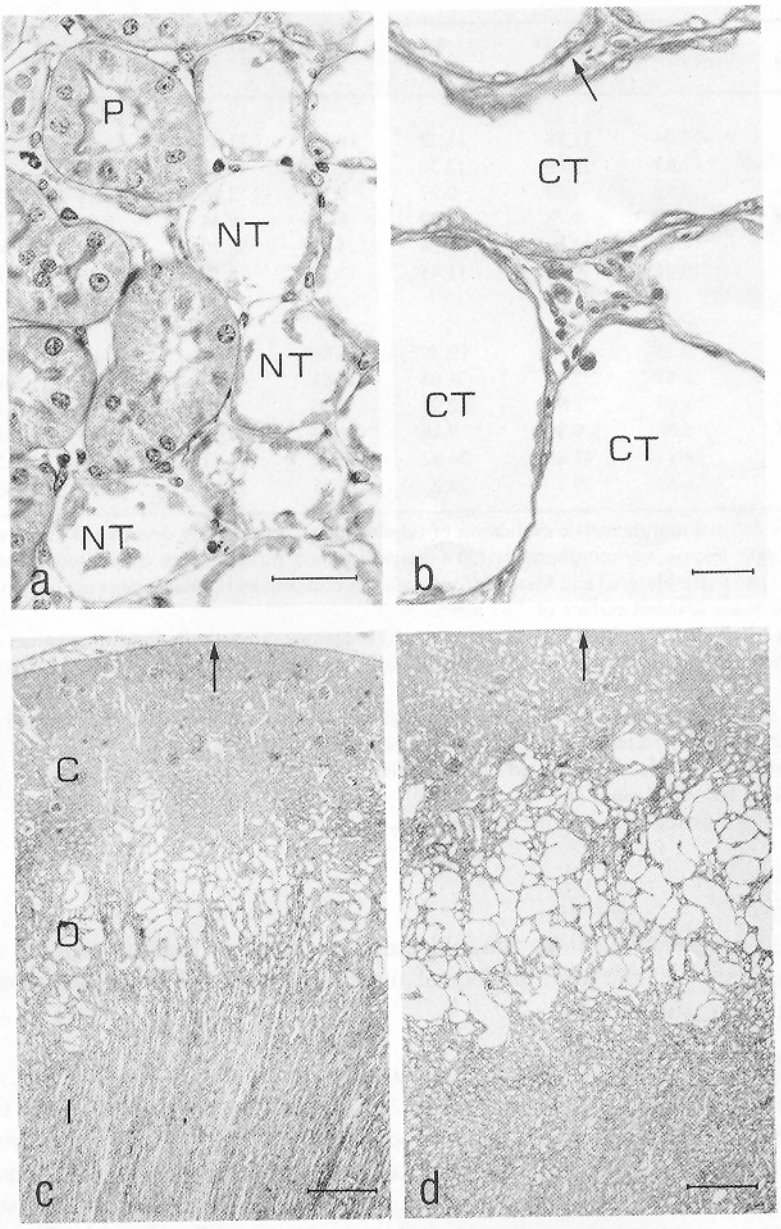

Fig. 1. Light micrographs (paraffin sections) of kidney tissue in rats treated with cisplatin (8 mg/kg) and sacrificed, respectively 4 days (a), 7 days (c), or 21 days (b,d) after the last drug injection. (a) Necrotic straight proximal tubules (NT) lined by a denuded basement membrane are present in OSOM. Desquamated cells can be seen in the lumina of necrotic tubules. Seemingly intact proximal tubules (P) are also present. (b) Clusters of cystic tubules (CT) characterized by a widely dilated lumen lined by a flattened epithelium and a thickening of basement membrane (arrows). (c,d) Sagittal sections of kidneys renal cortex (C), OSOM (O) and ISOM (I) showing the development of tubular cysts and the progression of cystic dilatations from OSOM to kidney cortex and ISOM. Arrows indicate the renal capsule. Scale bars = 20 μm (a,b) and 400 μm (c,d).

Table 1. Area density of tubular lumina

Time of sacrifice[a]	Controls	4 days	7 days	14 days	21 days	50 days	60 days
Cortex							
Mean[b]	12.04	11.78	13.32	19.23*	21.84*	18.45	25.57*
Median	11.83	10.86	13.30	19.74	19.24	17.87	25.91
S.E.	0.96	1.03	0.97	2.56	2.96	2.78	3.83
95% conf.[c]	3.07	3.28	3.09	8.16	9.44	8.86	12.19
Max[d]	14.29	14.87	15.24	24.22	30.70	24.55	34.12
Min[d]	10.21	10.55	11.45	13.23	18.18	13.50	16.33
OSOM							
Mean[b]	9.53	35.73*	29.30*	36.86*	50.65*	48.05*	48.47*
Median	8.67	35.69	28.05	35.81	49.96	49.78	49.99
S.E.	1.69	2.93	2.91	7.66	8.30	5.22	3.82
95% conf.[c]	5.38	9.34	9.28	24.39	26.43	16.63	12.16
Max[d]	14.11	41.83	36.92	52.92	69.43	58.77	55.75
Min[d]	6.67	29.7	24.2	23.05	33.24	33.88	38.15

Computer-assisted morphometric evaluation of tubular lumen area density determined on paraffin sections by light microscopy morphometry (50× magnification), using a video camera connected to the SAMBA system (see Material and Methods for details): % occupied by tubular lumina in cortex or OSOM on a total tissue scanned surface of 7.63 mm^2.

*The non-parametric Mann-Whitney U test was used to compare statistically individual values obtained from each experimental group ($n = 4$). The asterisks indicate values significantly different ($P < 0.05$) from controls.

[a]Treated animals were injected with cisplatin (8 mg/kg) and sacrificed 4–60 days after the end of treatment. Controls were treated with 0.9% NaCl and processed in parallel ($n = 4$).

[b]Mean area density value is calculated on 4 animals.

[c]Values for a 95% confidence interval.

[d]Limit values observed in each experimental group.

to 60 000 μm^2, equivalent to 500-fold the mean value of luminal tubular area in controls. However, the total number of these large cysts is limited compared with medium size cystic tubules.

Tridimensional reconstructions of cystic tubules

As shown in stereoscopic picture (Fig. 3a) and in Figs. 3b and 3c, cystic tubules reconstructed in OSOM show some circonvolutions. Fig. 3b also shows that the transition between the dilated segment and the nephron located just above and below occurs in an abrupt manner. The observation of paraffin sections selected among those used for the tridimensional reconstruction illustrated in Fig. 3 (b,c) reveals that the cystic part of the nephron (Fig. 4a) is flanked above by the proximal convoluted tubule (Fig. 4b) and below by a descending loop of Henle (Fig. 4c), a fact which allows one to identify the dilated segment as a straight proximal tubule. The part of the proximal convoluted tubule located just above the cystic dilatation displays histopathological alterations such as single-cell necrosis, loss of brush border and a thickening of the basement membrane (Fig. 4b) on a length of approx. 70 μm. Beyond this point the proximal convoluted tubule (Fig 4b) and glomerulus show a normal morphology. On the opposite site of cystic dilatation, the beginning

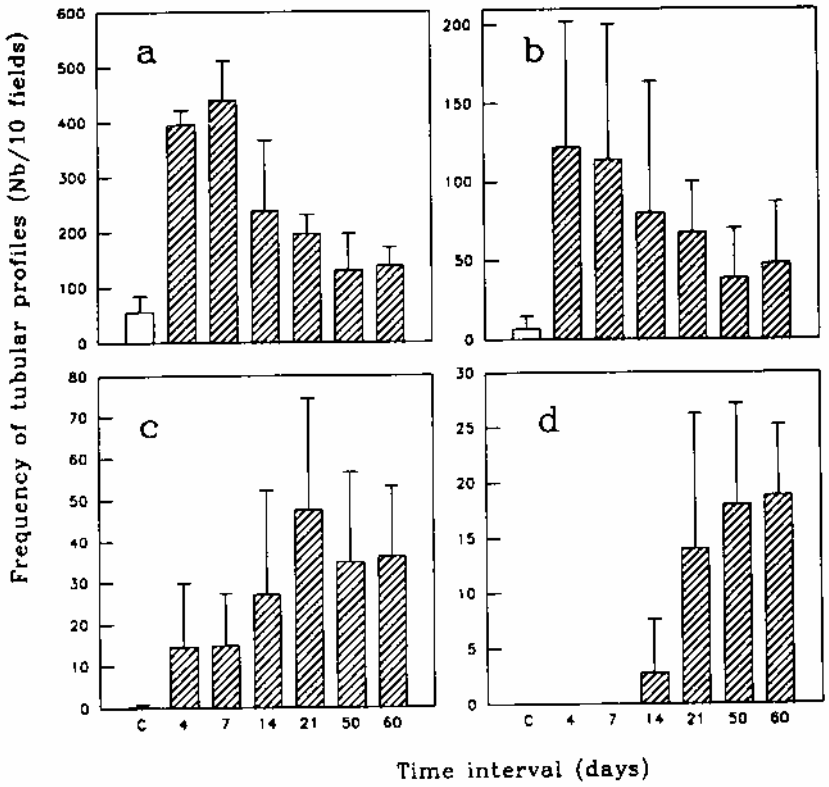

Fig. 2. Frequency of tubular profiles (luminal surface). The four histograms represent, for each experimental group, the incidence of tubular profiles with a luminal area ranging from 1000 to 4000 μm^2 (a); 4001 to 10 000 μm^2 (b); 10 001 to 30 000 μm^2 (c) and larger than 30 000 μm^2 (d). For each animal the average number of tubular profiles was evaluated in OSOM on a total surface of 7.63 mm^2 (see Material and Methods for details). Four animals per experimental group were used for the analysis and the data are expressed as means ± S.D. The abcissa gives, for each experimental group, the time interval after the last cisplatin injection. Some tubular profiles with an abnormally enlarged luminal area (1000 to 10 000 μm^2) were observed in control animals (C) and correspond to a few number of tubules sectioned obliquely or longitudinally.

of the descending loop of Henle is also altered and shows a wide lumen and a thickening of the basement membrane (Fig. 4c).

Compared with OSOM, the cystic tubules present in ISOM are less convoluted (Figs. 3d and 3e). The histological examination of the anterior and posterior poles of the cystic tubule appearing in Fig. 5 (a,c) indicates that this dilated tubule derives originally from a thin ascending loop of Henle or from a distal straight tubule or both, since the cystic tubule is limited on one side by an ascending loop of Henle (Fig. 5d) and on the opposite side by a distal straight tubule (Fig. 5b). Both structures present a thickening of the basal membrane.

In the kidney cortex, the spatial organization of cystic tubules shows more convolutions, as compared to those present in outer medulla. These cystic tubules most probably derive from proximal convoluted tubules. In contrast with cystic tubules

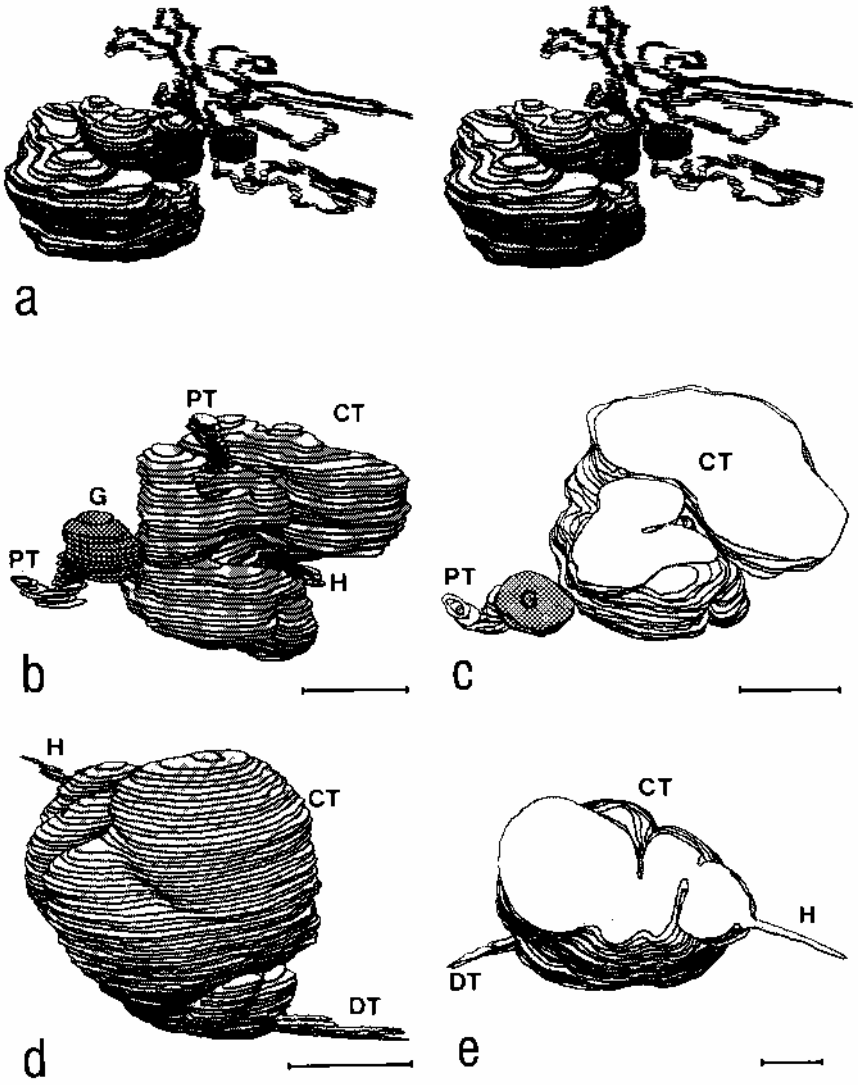

Fig. 3. Computer-assisted tridimensional reconstructions of cystic tubules, obtained from consecutive digitalized microscopic fields (see Material and Methods for details). Tridimensional analysis was performed on rats treated with cisplatin (8 mg/kg) and sacrificed 2 months after the end of treatment. (a) Stereoscopic view of cystic tubule localized in OSOM (same nephron as in Fig. 4). Cystic tubular dilatation shows some circonvolutions. The cystic segment shows a length of 900 μm and a maximum diameter of approx. 300 μm. Proximal convoluted portion (segments S1 and S2) of the same nephron and its glomerulus (cross-hatched area) can also be seen in three dimensions. The length of proximal convoluted tubule is 5200 μm and the diameter of glomerulus approx. 125 μm. (b) Tridimensional reconstruction of the same cystic tubule after a 180° rotation. This view shows the connections between cystic segment (CT) and a descending Henle's loop (H) and also between the cystic tubule and a proximal convoluted tubule (PT). Glomerulus (G) appears as a size reference. (c) Diagram of the same tubule partially reconstructed. (d) Tridimensional reconstruction of a cystic tubule localized in ISOM (same nephron as in Fig. 5). This view shows the transition between cystic dilatation (CT) and the loop of Henle (H) and the connection with a distal tubule (DT). As shown on the partially reconstructed diagram in e, the cystic tubular dilatation is straighter than in OSOM. Scale bars = 200 μm.

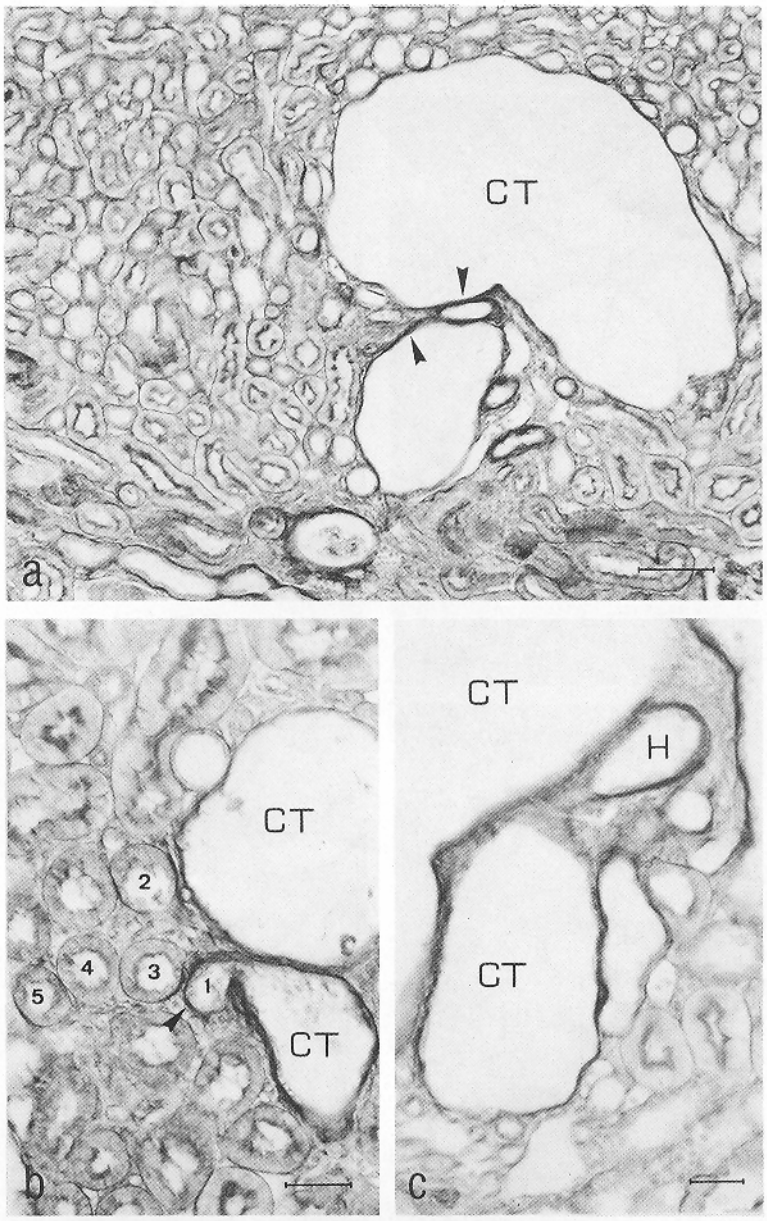

Fig. 4. Light microscope appearance of cystic tubule submitted to tridimensional analysis (Figs. 3a–3c). (a) The cystic tubule (CT) is located in OSOM and characterized by a flattened epithelium lined by a thick basement membrane (arrow heads). The transition between cystic segment and proximal convoluted tubule can be seen in Fig. 3b. The segment of proximal convoluted tubule located just before cystic dilatation (tubular sections 1 and 2) shows morphological alterations such as cell necrosis, loss of brush border and an important thickening of the basement membrane (arrow head). Tubular profiles corresponding to a more proximal portion of the same nephron (tubular sections 3–5), thus more distant from cystic dilatation, show a normal morphology. (c) Transition between cystic tubule (CT) and the beginning of the descending loop of Henle (H). Scale bars = 100 μm (a), 40 μm (b) and 30 μm (c).

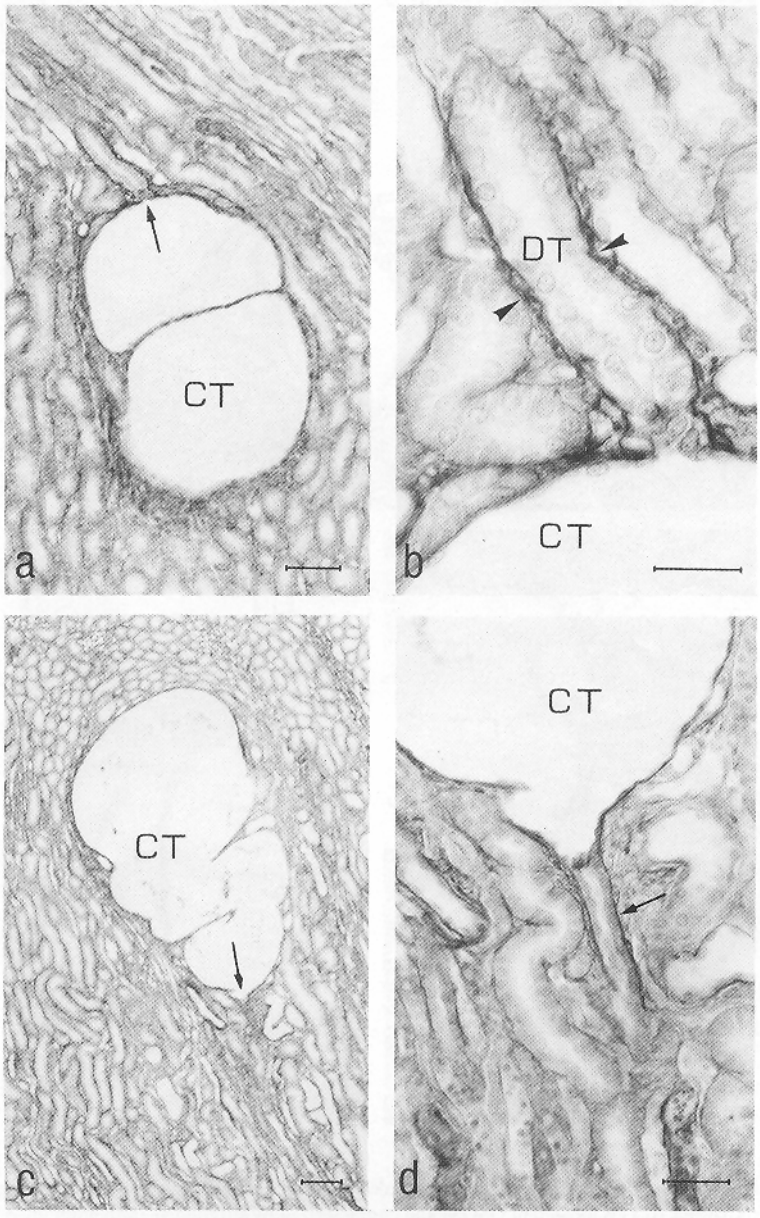

Fig. 5. Light microscope appearance of tridimensional cystic tubule in Fig. 3 (d,e). (a,c) Low magnification of a cystic tubule (CT) located in the inner stripe of outer medulla (ISOM). Arrows point to the junctions with the non-cystic parts of the nephron. (b) High magnification of the top pole of cystic tubule (CT). The distal straight tubule (DT), in continuity with the cystic dilatation, shows a thickening of the basement membrane (arrow heads). (d) High magnification of the transition between cystic tubule (CT) and the thin ascending loop of Henle (arrow). Scale bars = 100 μm (a,c), 20 μm (b) and 40 μm (d).

located in outer medulla, cortical cystic tubules are less dilated with a maximum diameter < 100 μm (data not shown).

Discussion

The dosage of cisplatin (8 mg/kg) used in this study is within the range administered in clinical practice [15,21]. Under these experimental conditions, cisplatin rapidly induces an acute tubular necrosis affecting principally S3 segments. In addition to necrotic injury, the most typical alteration encountered in cisplatin-treated rats consists of a progressive cystic tubular degeneration primarily involving tubules located in OSOM. Two months after cisplatin administration, these cystic tubules are no longer restricted to OSOM but progress into kidney cortex and ISOM. This time interval has thus been chosen to compare, by spatial reconstructions, the structure and origin of cystic tubules present in these three zones of the kidney.

The morphometric study of cyst development in rat kidney largely confirms qualitative morphological observations reported in previous studies [7,12–14,18,20]. The tissue area occupied by cystic tubules reaches a maximum 3 weeks after the end of the treatment. Our quantitative data show that the number of altered tubules in OSOM remains approximately the same during the whole period of observation. This result suggests that the cystic expansion results of a progressive dilatation of primarily altered tubules. After 2 months, despite the fact that the total cystic area is stabilized, some cystic tubules continue to increase in size. This apparent contradiction probably arises from a slow reversal of some tubules to normal morphology whereas cystic dilatation is still in progress in other tubules [20,29,30].

Cystic diseases of kidney are common pathologies present in approx. 10% of all end-stage renal diseases [16]. Recent studies on the etiology of renal tubular cystic degeneration show two major causes. On the one hand, some renal cysts are hereditary in nature [16,39]. On the other hand, cystic tubular dilatations can be induced by the administration of nephrotoxic compounds such as 2-amino-4,5-diphenyl thiazole [3], lithium chloride [17] or cisplatin [14,20]. Depending on the etiology (inherited versus acquired) and the nature of the causative agent, cystic degeneration can affect different portions of the nephron.

Previous studies suggest that cisplatin-induced cysts derive from proximal straight tubules [13,14,20,23]. This is largely confirmed by our tridimensional reconstructions of cystic tubules. Indeed, all cystic tubules analysed in OSOM were identified as S3 segments. The anatomical localization of the tubular cystic dilatations appears consistent with the intrarenal distribution of cisplatin. The observation of kidney sections, after injection of [^{195m}Pt]cisplatin followed by histoautoradiography, demonstrate a preferential accumulation of cisplatin within proximal straight tubules [36]. Some authors suggest that drug accumulation in this part of the nephron results from an active transport into the epithelium through the organic cation transport [34,35,40].

Some studies suggest that tubular dilatation of S3 segment leads to the atrophy or disappearance of the corresponding nephrons with formation of atubular glomeruli [23]. Our observations on convoluted proximal tubules and glomeruli belonging to nephrons undergoing cystic dilatation does not confirm this hypothesis. Although we have observed histopathological alterations in tubular sections directly connected with cystic tubules, these alterations disappear rapidly along the nephron.

Thus, in affected nephrons proximal convoluted tubules and glomeruli remain mostly intact and probably continue to assume physiological functions.

In contrast with previous studies, cystic tubules reconstructed in ISOM reveal that cisplatin-induced cystic degeneration in rat kidney is not restricted to proximal straight tubules but can also appear in the long term in distal straight tubules and/or in loops of Henle. Some authors have observed moderate histopathological alterations in these segments soon after cisplatin exposure [2,9,20], but no cyst formation. The late development of cystic dilatation in this part of the nephron could be due to some cisplatin accumulation in distal tubules in addition to S3 segments. The cystic degeneration of distal tubules might play a role in the chronic hypokalaemia and hypocalciuria (Gitelman's syndrome) found in animals and patients treated with cisplatin [1,22].

The pathogenesis of cystic tubules remains largely unknown, although three distinct factors have been identified as critical components in the development of renal cysts. First an important cellular proliferation is present prior to cystic degeneration. In previous studies [20,28–31], our group showed a rapid increase of cell proliferation in S3 segments, occurring before cystic degeneration. A cell hyperplasia, albeit moderate, has also been detected in distal tubules [20] and could lead to a late cystic expansion of this tubule. Secondly an accumulation of fluid within the nascent cyst could be responsible for the progressive dilatation of the altered tubule. However intratubular pressure is not always present as a causative factor. Indeed, studies performed on proximal tubule cells in cultures exposed to cisplatin have demonstrated the formation of cystic dilatations in absence of intra-tubular fluid pressure [37]. Moreover, structural modifications of the tubule basement membrane of cystic tubule may play an prominent role in the development of this alteration [3–5,16,26]. Abnormal basement membrane components have been attributed to defective gene expression. Cisplatin is well known to produce covalent adducts in the DNA molecule [8,11]. High concentrations of this compound in renal tubular cell might disturb normal DNA transcription and most probably induce abnormalities in the proteins of the basement membrane. In our study we have shown that abnormal morphology of the basement membrane is not only restricted to the cystic part but is also present in tubular segments in continuity with cystic tubules. However the thickening of the basement membrane progressively becomes less apparent when the distance increases from the tubular cysts. This observation suggests that an alteration of the basement membrane occurs as a prerequisite to the cystic dilatation and might play a major role in the pathogenesis of cisplatin-induced renal cysts.

Acknowledgements

This study received financial support from the Fund for Medical Scientific Research (Belgium) (Grant no. 3.4551.86). G. Laurent is Research Associate of the Belgian National Fund for Scientific Research. D. Nonclercq is the recipient of a fellowship from the National Fund for Scientific Research ('Télévie 1991'). We thank Mr. J. Noël for his skilled technical assistance.

References

1 Bianchetti MG, Kanaka C, Ridolfi-Lüthy A, Wagner HP, Hirt A, Paunier L, Peheim E, Oetliker OH. Chronic renal magnesium loss, hypocalciuria and mild hypokalaemic metabolic alkalosis after cisplatin. Pediatr Nephrol 1990;219–222.

2 Bompart G, Orfilla C, Girolami J-P. Distal nephrotoxicity of cisplatin demonstrated by urinary kallikrein excretion and morphological study in rat. Toxicology 1991;69:121–132.
3 Carone FA, Hollenberg PF, Nakamura S, Punyarit P, Glogowski W, Flouret G. Tubular basement membrane change occurs pari passu with the development of cyst formation. Kidney Int 1989;35:1034–1040.
4 Carone FA, Hong J, Nakamura S, Liu Z, Kanwar Y. Synthesis, transport and matrix assembly of proteoglycans by human cyst-derived cells. Seventh international symposium of nephrology at Montecatini. Kidney, Proteins and Drugs (abstract). Montecatini, Italy, October 1991; 1.
5 Carone FA, Nakamura S, Punyarit P, Kanwar Y. Sequential tubular cell and membrane changes in polycystic disease. Seventh international symposium of nephrology at Montecatini. Kidney, Proteins and Drugs (abstract). Montecatini, Italy, October 1991;2.
6 Choie DD, Langnecker DS, del Campo AA. Acute and chronic cis-platin nephrotoxicity in rat. Lab Invest 1981;44:397–402.
7 Chopra S, Kaufman JS, Jones TW, Hong WK, Gehr Mk, Hamburger RJ, Flamenbaum W, Trump BF. Cis-diamminedichloroplatinum-induced acute renal failure in the rat. Kidney Int 1982;21: 54–64.
8 Ciccarelli RB, Solomon MJ, Varshavsky A, Lippard CJ. In vivo effects of cis- and trans-diamminedichloroplatinum (II) on SV40 chromosomes: differential repair, DNA-protein cross-linking, and inhibition of replication. Biochemistry 1985;24:7533–7540.
9 Daugaard G, Abilgaard U, Larsen S, Holstein-Rathlou NH, Amtorp O, Olesen HP, Leyssac PP. Functional and histopathological changes in dog kidney after administration of cisplatin. Renal Physiol 1987;10:54–64.
10 Daugaard G, Abildgaard U. Cisplatin nephrotoxicity. Cancer Chemother Pharmacol 1989;25:1–9.
11 Dijt FJ, Fichtinger-Schepman AM, Berends F, Reedijk J. Formation and repair of cisplatin-induced adducts to DNA in cultured normal and repair-deficient human fibroblasts. Cancer Res 1988;48:6058–6062.
12 Dobyan DC, Levi J, Kosek J, Weiner MW. Mechanism of cis-platinum nephrotoxicity: II. Morphologic observations. J Pharmacol Exp Ther 1980;213:551–556.
13 Dobyan DC, Hill D, Lewis T, Bulger RE. Cyst formation in rat kidney induced by cis-platinum administration. Lab Invest 1981;45:260–268.
14 Dobyan DC. Long-term consequences of cis-platinum-induced renal injury: a structural and functional study. Anat Rec 1985;212:339–245.
15 Gandara DR, Perez EA, Phillips WA, Lawrence HJ, De Gregorio M. Evaluation of cisplatin dose intensity: current status and future prospects. Anticanc Res 1989;9:1121–1128.
16 Gardner KD. Cystic kidneys. Kidney Int 1988;33:610–621.
17 Hestbech J, Hansen HE, Amdisen A, Olsen S. Chronic renal lesions following long-term treatment with lithium. Kidney Int 1977;12:205–213.
18 Jones TW, Chopra S, Kaufman JS, Flamenbaum W, Trump BF. Cis-diamminedichloroplatinum II-induced acute renal failure in the rat. Lab Invest 1985;52:363–374.
19 Kriz W, Bankir L, Bulger RE, Burg MB, Goncharevskaya OA, Imai M, Kaissling B, Maunsbach AB, Moffat DB, Morel F, Morgan TO, Natochin YV, Tischer CC, Venkatachalam MA, Whittembury G, Wright FS. A standard nomenclature for structures of the kidney. Kidney Int 1988;33:1–7.
20 Laurent G, Yernaux V, Nonclercq D, Toubeau G, Maldague P, Tulkens PM, Heuson-Stiennon J-A. Tissue injury and proliferative reponse induced in rat kidney by cis-diamminedichloroplatinum II. Virchows Arch B Cell Pathol 1988;55:129–145.
21 Loehrer PJ, Einhorn LH. Diagnosis and treatment. Drugs five years later: cisplatin. Ann Int Med 1984;100:704–713.
22 Magil MB, Mavichak V, Wong NL, Quamme GA, Dirks JH, Sutton RA. Long-term morphological and biological observations in cisplatin-induced hypomagnesemia in rats. Nephron 1986;43:223–230.
23 Marcussen N, Jacobsen NO. The progression of cisplatin-induced tubulointerstitial nephropathy in rats. APMIS 1992;100:256–268.
24 Mavichak V, Wong NL, Quamme GA, Magil AB, Sutton RA, Dirks JH. Studies on the pathogenesis of cisplatin-induced hypomagnesemia in rats. Kidney Int 1985;28:914–921.
25 Meijer D, Sleijfer DT, Mulder NH, Donker AJ. Cisplatin induced nephrotoxicity. Neth J Med 1982;25:262–269.
26 Neufeld TK, Douglass D, Grant M, Ye M, Silva F, Nadasdy T, Grantham JJ. In vitro formation

and expansion of cysts derived from human renal cortex epithelial cells. Kidney Int 1992;4:1222–1236.
27 Nichols CR, Loehrer PJ, Greist A, Kubilis PS, Hoffman R. Salvage chemotherapy for lymphoma with VP-16, ifosfamide and cisplatin. Med Pediatr Oncol 1988;16:12–16.
28 Nonclercq D, Toubeau G, Laurent G, Tulkens PM, Heuson-Stiennon J-A. Nephrotoxic injury and renal tissue repair associated with the administration of the anticancer drugs cisplatin and carboplatin. Micron Microscopica Acta 1989;20:51–58.
29 Nonclercq D, Toubeau G, Laurent G, Tulkens PM, Heuson-Stiennon J-A. Tissue injury and repair in the rat kidney after exposure to cisplatin and carboplatin. Exp Mol Pathol 1989;51:123–140.
30 Nonclercq D, Toubeau G, Tulkens P, Heuson-Stiennon J-A, Laurent G. Renal tissue injury and proliferative response after successive treatments with anticancer platinum derivatives and tobramycin. Virchows Archiv B Cell Pathol 1990;59:143–158.
31 Nonclercq D, Toubeau G, Lambricht P, Heuson-Stiennon J-A, Laurent G. Redistribution of Epidermal growth factor immunoreactivity in renal tissue after nephrotoxin-induced tubular injury. Nephron 1991;57:210–215.
32 Peckham MJ, Horwich A, Hendry WF. Advanced seminoma: treatment with cis-platinum-based combination chemotherapy or carboplatin (JM8). Br J Cancer 1985;52:7–13.
33 Prestayko AW. Cisplatin and analogues: a new class of anti-cancer drugs. In: Crooke ST, Prestayko AW, eds. Cancer and chemotherapy, vol. III, antineoplastic agents. Academic Press, New York 1981;133–154.
34 Roth BJ, Greist A, Kubilis PS, Williams SD, Einhorn LH. Cisplatin-based combination chemotherapy for disseminated germ cell tumors: long-term follow-up. J Clin Oncol 1988;6:1239–1247.
35 Safirstein R, Winston J, Guttenplan G. Cisplatin nephrotoxicity: physiological and biochemical aspects. In: McBrien DCH, Slater TF, eds. Biochemical mechanisms of platinum antitumour drugs. I.R.L. Press Limited, Oxford 1986;271–306.
36 Safirstein R, Winston J, Moel D, Dikman S, Guttenplan J. Cisplatin nephrotoxicity: insights into mechanism. Int J Androl 1987;10:325–346.
37 Tay LK, Bregman CL, Masters BA, Williams PD. Effect of cis-diamminedichloroplatinum (II) on rabbit kidney in vivo and on rabbit renal proximal tubule cells in culture. Cancer Res 1988;48:2538–2543.
38 Walker EM, Gale GR. Methods of reduction of cisplatin nephrotoxicity. Ann Clin Lab Sci 1981;38:535–547.
39 Wilkinson JE, Woychik R, Godfrey VL, Moyer J. The TG 737 mouse: an animal model of autosomal recessive polycystic kidney disease (abstract). FASEB J 1992;6:A1348.
40 Williams PD, Hottendorf GH. Effect of cisplatin on organic ion transport in membrane vesicles from rat kidney cortex. Cancer Treat Rep 1985;69:875–880.
41 Wong NL, Sutton RA, Dirks JH. Effect of cisplatin on straight tubule transport of divalent cations in the rabbit. Nephron 1988;49:62–66.